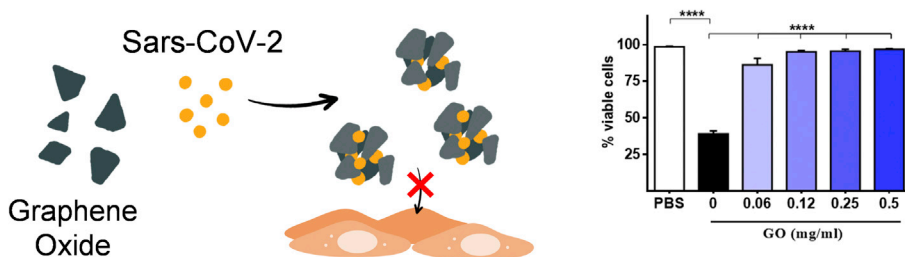


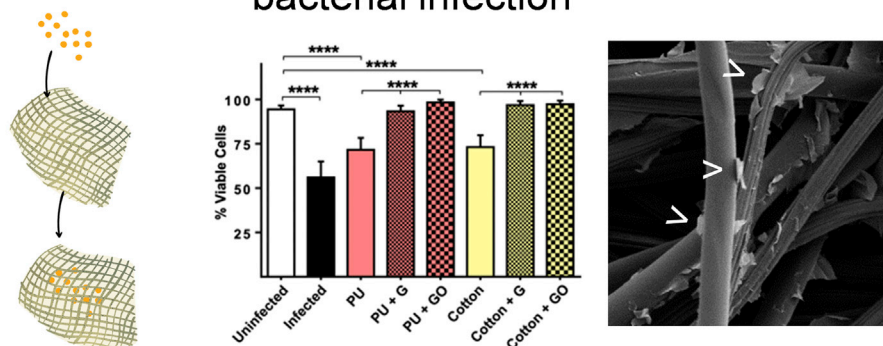
Article

Graphene nanoplatelet and graphene oxide functionalization of face mask materials inhibits infectivity of trapped SARS-CoV-2

Graphene Oxide in solution traps Sars-CoV-2 and viability of VERO cells is restored



Graphene functionalized fabrics inhibits viral and bacterial infection



Flavio De Maio, Valentina Palmieri, Gabriele Babini, ..., Patrick Soon-Shiong, Michela Sali, Massimiliano Papi

valentina.palmieri@cnr.it

Highlights

Graphene oxide (GO) traps Sars-CoV-2 particles in liquid medium

Cotton or polyurethane can be functionalized with graphene or GO nanoparticles

Infection is inhibited when Sars-CoV-2 contacts with functionalized fabrics

Graphene-functionalized fabrics are effective against bacteria and are biocompatible



Article

Graphene nanoplatelet and graphene oxide functionalization of face mask materials inhibits infectivity of trapped SARS-CoV-2

Flavio De Maio,^{1,2} Valentina Palmieri,^{3,*} Gabriele Babini,⁴ Alberto Augello,^{5,6} Ivana Palucci,^{1,2} Giordano Perini,^{5,6} Alessandro Salustri,² Patricia Spilman,⁷ Marco De Spirito,^{5,6} Maurizio Sanguinetti,^{1,2} Giovanni Delogu,^{2,8} Laura Giorgia Rizzi,⁹ Giulio Cesareo,⁹ Patrick Soon-Shiong,¹⁰ Michela Sali,^{1,2,11} and Massimiliano Papi^{5,6,11,12}

SUMMARY

Recent advancements in bidimensional nanoparticles production such as graphene (G) and graphene oxide (GO) have the potential to meet the need for highly functional personal protective equipment (PPE) against SARS-CoV-2 infection. The ability of G and GO to interact with microorganisms provides an opportunity to develop engineered textiles for use in PPE and limit the spread of COVID-19. PPE in current use in high-risk settings for COVID transmission provides only a physical barrier that decreases infection likelihood and does not inactivate the virus. Here, we show that virus pre-incubation with soluble GO inhibits SARS-CoV-2 infection of VERO cells. Furthermore, when G/GO-functionalized polyurethane or cotton was in contact SARS-CoV-2, the infectivity of the fabric was nearly completely inhibited. The findings presented here constitute an important innovative nanomaterial-based strategy to significantly increase PPE efficacy in protection against the SARS-CoV-2 virus that may implement water filtration, air purification, and diagnostics methods.

INTRODUCTION

The emergence of the severe acute respiratory syndrome coronavirus 2 (SARS-CoV-2) and the resultant coronavirus infectious disease 2019 (COVID-19) pandemic has prompted the ubiquitous use of face masks (Clase et al., 2020; Feng et al., 2020; Sommerstein et al., 2020; Sunjaya and Jenkins, 2020; Palmieri et al., 2021) to curb transmission in clinical, public, and working contexts. A global shortage of medical-grade masks such as N95 masks has resulted in the widespread use of cloth masks, including woven cotton masks, to reduce airborne transmission (Clase et al., 2020). Although these masks offer some protection against viral transmission, there is a continuing high demand for personal protective equipment (PPE). In particular, owing to the inability to avoid or difficulty in isolation of infectious persons who are contagious during the initial days of infection when symptoms are mildest or not present (Arons et al., 2020; Liu et al., 2020), masks and PPE with better protective characteristics are needed.

Design of a protective surgical face mask consists of the use of materials with different roles and properties, layered in a sequence to optimize functionality. The first layer, in contact with the skin of the wearer, allows droplets to pass through and be absorbed in the adjacent hydrophilic layer, thereby keeping the skin dry (Sarkar et al., 2020). This second hydrophilic layer also absorbs and holds microorganisms in the mask, limiting their ability to spread to other people.

In contrast, the outside layer of the mask is typically a hydrophobic non-woven tissue sheet. Its low wettability prevents the escape of fluids from the middle layer to the outside and at the same time stops entry of droplets from the exterior.

To improve the protective properties of masks, nanomaterials scientists have proposed integration of virus-inactivating properties with standard propylene- and cloth-filtering properties with the goal of developing improved PPE (O'Dowd et al., 2020; Palmieri and Papi, 2020; Raghav and Mohanty, 2020; Sportelli et al., 2020; Weiss et al., 2020; Ziem et al., 2017).

¹Dipartimento di Scienze di Laboratorio e Infettivologiche, Fondazione Policlinico Universitario "A. Gemelli" IRCSS, Largo A. Gemelli, 8 00168 Rome, Italy

²Dipartimento di Scienze Biotecnologiche di Base, Cliniche Intensivologiche e Perioperatorie – Sezione di Microbiologia, Università Cattolica del Sacro Cuore, Largo Francesco Vito 1, Rome 00168, Italy

³Istituto dei Sistemi Complessi, CNR, Via dei Taurini 19, 00185 Rome, Italy

⁴Dipartimento Scienze della Salute della Donna, del Bambino e di Sanità Pubblica, Fondazione Policlinico Universitario "A. Gemelli", Largo A. Gemelli, 8 00168 Rome, Italy

⁵Dipartimento di Neuroscienze, Università Cattolica del Sacro Cuore, Largo Francesco Vito 1, Rome 00168, Italy

⁶Fondazione Policlinico Universitario "A. Gemelli" IRCSS, Largo A. Gemelli, 8 00168 Rome, Italy

⁷ImmunityBio, LLC, Culver City, 440 Duley Road, El Segundo, California, CA 90245, USA

⁸Mater Olbia Hospital, Strada Statale 125 Orientale Sarda, 07026 Olbia SS, Italy

⁹Directa Plus S.p.A. c/o ComoNEXt - Science and Technology Park, 22074 Lomazzo, Como, Italy

¹⁰Nantworks LLC, Culver City, 9920 Jefferson Boulevard, California, CA 90230, USA

¹¹Co-senior authors

¹²Lead contact

*Correspondence: valentina.palmieri@cnr.it
<https://doi.org/10.1016/j.isci.2021.102788>



In recent years, the bidimensional material graphene nanoplatelet (G) and its derivatives have captured much attention owing to their interactions with microorganisms (Valentini et al., 2016; Shams et al., 2017; Matharu et al., 2020). Pristine G is a single-atom-thick sheet of hexagonally arranged carbon atoms (Bourque and Rutledge, 2018), whereas graphene oxide (GO) is its oxidized form. Being a single layer of atoms, G has an exceptionally high surface area and interacts uniquely with organisms with sizes in the order of hundreds of nanometers, i.e., bacteria and viruses (Palmieri and Papi, 2020). GO oxygen groups make the surface more hydrophilic compared with G (Palmieri et al., 2017a; Kumar and Parekh, 2020).

It has been demonstrated that bacteria that come into contact with the G surface lose integrity (Palmieri et al., 2017a, 2017c) and that G has good viral inhibition capacity (Ziem et al., 2016). Graphene interacts directly with viruses mainly by hydrogen bonding, electrostatic interactions, and redox reactions (Song et al., 2015), and many G-derived materials have an intrinsic ability to adsorb charged lipids and destroy membranes (Frost et al., 2012; Rui et al., 2015; Chen et al., 2016), suggesting a likely interaction with enveloped viruses like SARS-CoV-2. Furthermore, G itself can be additionally functionalized with anti-viral particles and drugs (Akhavan et al., 2012; Ziem et al., 2016, 2017; Yang et al., 2017; Palmieri et al., 2018; Donskyi et al., 2019; Naskalska et al., 2019; Jones et al., 2020).

In the last months, it has been evidenced how G and G-related products could improve face masks performance and recycling process or could be embedded as sensing material for viruses in textiles (Kumar et al., 2020; Lin et al., 2020; Palmieri and Papi, 2020; Raghav and Mohanty, 2020; Srivastava et al., 2020; Tabish and Hamblin, 2020; Zhong et al., 2020), but the effects of G and GO either in solution or embedded in fabrics for PPE on Sars-CoV-2 have not been quantified experimentally.

To verify the SARS-CoV-2 inhibition by G-related nanomaterials, we first investigated the ability of GO in solution (owing to its relative hydrophilicity) to bind and entrap suspended SARS-CoV-2 viral particles. We found that pre-incubation of virus with GO nearly completely suppressed infectivity in the commonly used VERO cell model of SARS-CoV-2 infection. Then we showed the potential to exploit the interaction of graphene with viruses in the fabrication of masks by testing the efficacy of G and GO functionalization of cotton and non-woven, polyurethane (PU) material. We found that virus filtration through either G- or GO-functionalized cotton or PU also almost wholly eradicated SARS-CoV-2 infectivity. Finally, because protection against bacterial infection is also desirable for face mask materials (Zhiqing et al., 2018), as biocompatibility, we tested the materials functionalized with G or GO for their antibacterial effects against *E. coli* and effects on viability of the eukaryotic cell line. We found that the functionalized materials showed antibacterial effects but did not affect eukaryotic cell viability.

On the whole, a plethora of applications of G and GO are presented in this work.

RESULTS AND DISCUSSION

In the first experimental setting, the ability of GO in solution to trap SARS-CoV-2 and reduce infectivity in VERO cells was assessed. SARS-CoV-2 viral particles at a concentration of $\sim 10^5$ particles/mL were incubated with increasing concentrations of GO for 2 h. Following incubation, solutions were centrifuged and supernatants were used to infect VERO cells to measure the infectivity of the virus (Figure 1A). Controls were treated with centrifuged viral solutions without GO.

Incubation of SARS-CoV-2 viral particles in suspension with GO reduced viral infectivity even at the lowest concentration of GO (0.06 mg/mL) as reflected by the cell density observed (Figure 1B). On the contrary, infected cells with exposure to SARS-CoV-2 without GO show only $\sim 40\%$ viability. GO therefore significantly reduced the load of viral particles. In Figure 1C, immunofluorescent labeling with anti-SARS-CoV-2 spike protein antibody is shown, and quantification is reported in Figure 1E confirming results visible by light microscopy. GO reduced cytotoxicity of SARS-CoV-2 viral particles as measured by both crystal violet staining (images in Figure 1D and quantification in Figure 1F) and lactate dehydrogenase release quantification (Figure 1G). No significant decrease of viral infectivity was observed without centrifuging the infection solution. These data demonstrate that water-soluble GO interacts with SARS-CoV-2 viral particles, entraps viruses causing precipitation in the pellet. This GO trapping reduces viral infectivity, in the *in vitro* live virus model of SARS-CoV-2 infection of VERO cells.

The trapping of microbial species is a mechanism known for bacteria and is caused by the propensity of GO surface to interact with lipidic membranes, like SARS-CoV-2 virus. Therefore, as occurs with bacterial

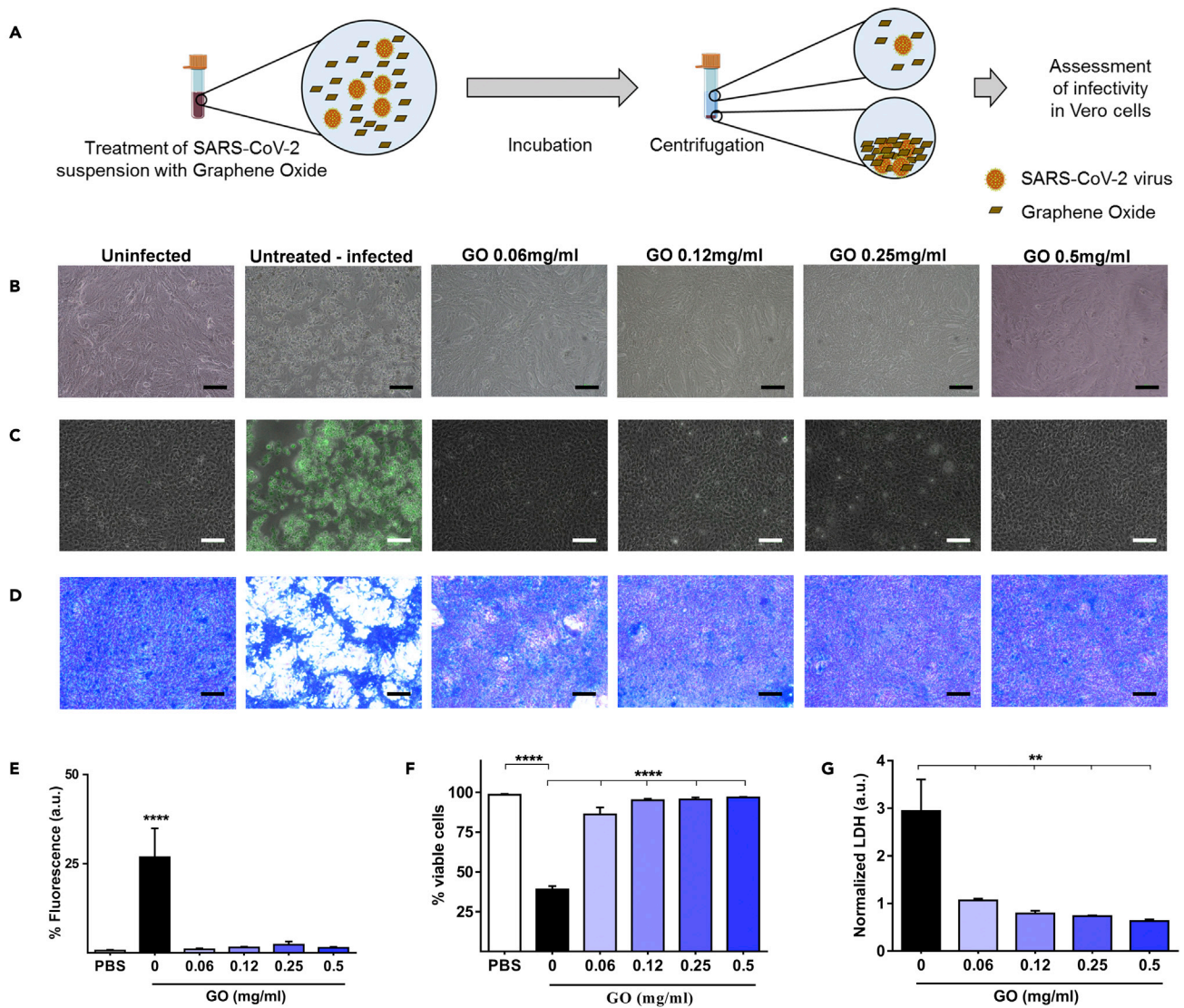


Figure 1. Graphene oxide (GO) entraps the SARS-CoV-2 virus and prevents infection

(A) A schematic representation of the experimental design to assess the ability of GO to trap virus in solution is shown. A SARS-CoV-2 clinical isolate was suspended in phosphate-buffered saline (PBS) at $\sim 10^5$ virus particles/mL and incubated with increasing concentrations of GO (0.06, 0.12, 0.25, and 0.5 mg/mL) or without GO (untreated) as positive control. Two hours later, GO was removed by centrifugation and supernatants were used to infect VERO cells. (B) Representative images of VERO cell density taken at 72 h are shown for uninfected cells, SARS-CoV-2-infected cells without GO, and infected cells with medium incubated with increasing concentrations of GO.

(C) Fluorescent microscopic images are shown for VERO cells labeled with an anti-viral spike (S) protein antibody under the same conditions as in (B)

(D–F) (D) Cell viability was also assayed with crystal violet staining, (E) fluorescence, and (F) crystal violet quantification of infected cells and cytotoxicity, respectively.

(G) Lactate dehydrogenase (LDH) was quantified in the cell supernatants to measure SARS-CoV-2-mediated cytotoxicity. Scale bars in B, C, and D are 50 μ m. Data are represented as mean \pm SD. Statistically significant results are indicated with “*” according to p value (**p < 0.01; ****p < 0.0001).

species, we hypothesize that the surface of GO entraps viral particles, possibly favored by the bridging of cations of cell medium (Palmieri et al., 2017a), causing a lack of infection of VERO cells.

To assess if functionalization of cotton material or PU is feasible and can result in better protection against viral penetration, we integrated G or GO into these materials. The functionalized materials were then imaged by scanning electron microscopy (SEM). As seen in Figure 2, SEM imaging reveals platelets of G or GO distributed on fibers that are particularly apparent on PU.

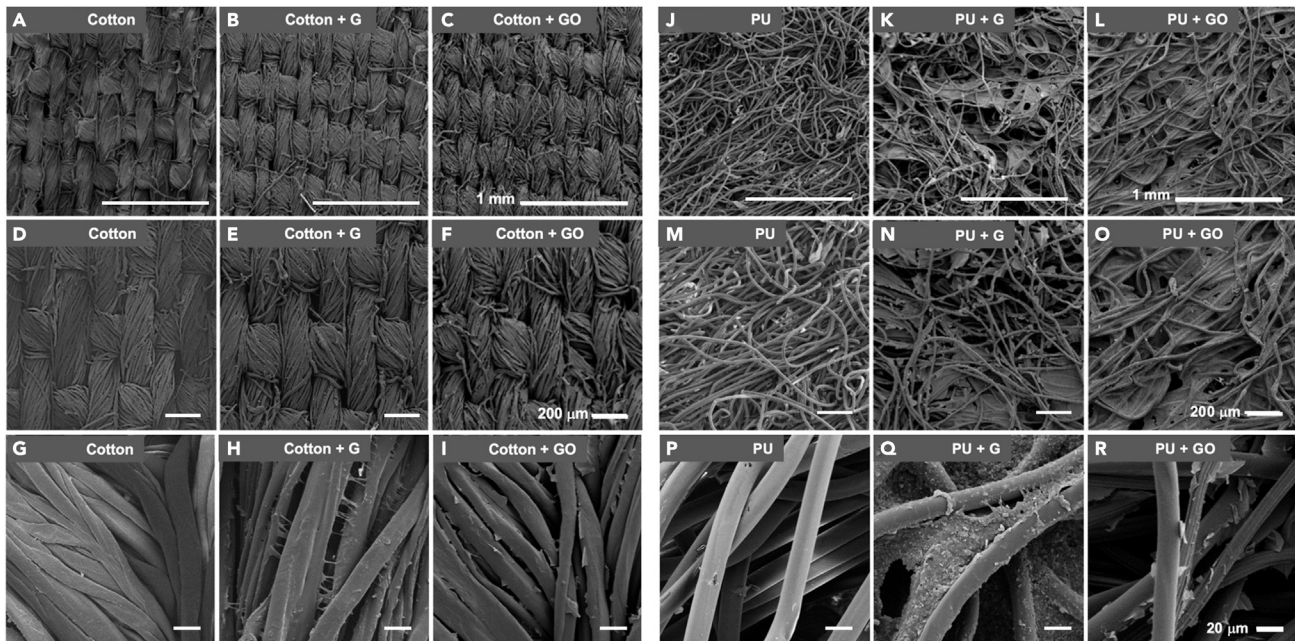


Figure 2. Scanning electron microscopic (SEM) images of graphene (G)- and graphene oxide (GO)-functionalized materials

Representative SEM images of cotton, cotton + G, and cotton + GO at 60X (A, B, and C, respectively), 100 X (D, E, and F, respectively), and 750X (G, H, and I, respectively) are shown. Similar images are shown for PU, PU + G, and PU + GO at 60X (J, K, and L, respectively), 100X (M, N, and O, respectively), and 750X (P, Q, and R, respectively). Scale bar is 1 mm in A–C and J–L, 200 μm in D–F and M–O, and 20 μm in G–I and P–R.

Two experimental paradigms were then used to test the potential for protection against SARS-CoV-2 infection by functionalized materials: static incubation and flow filtration.

The static and flow experimental designs are shown in [Figure S1](#).

In the static testing paradigm, viral particles suspended in medium were put in contact with G- or GO-functionalized materials for 2 h. Then the materials were washed with cell medium to recover particles from the fabric and the medium was used to treat VERO cells ([Figure S1A](#)). The cytotoxic effect of virus on VERO cell viability as seen by crystal violet staining ([Figure 3](#)) is greatly reduced by incubation of virus on PU or cotton functionalized with either G or GO as compared with non-functionalized materials ([Figures 3A–3D](#)). The quantitative analysis revealed that either G or GO integration into both materials confers statistically significant inhibition ([Figure 3E](#)).

For the flow filtration, the viral suspension was filtered through materials used as membranes in a custom 3D printed fabric holder ([Figures S1B–S1D](#)). SARS-CoV-2 suspensions were filtered through each material with or without G/GO functionalization and eluates were collected and used to infect VERO cells.

Just as with static incubation, integration of G or GO into either of the test materials resulted in a significant decrease in viral cytotoxicity that can be seen in images of crystal violet-stained cells ([Figures 3F and 3G](#)). The protection against virus-induced cell death was highly significant for both G- and GO-functionalized PU or cotton ([Figure 3H](#)).

In [Table 1](#), we calculated for each type of functionalized material the viral load reduction.

To confirm that the functionalized materials are biocompatible and not cytotoxic, A549 and VERO cells were incubated with cell culture medium exposed to graphene-functionalized materials. No decrease in cell viability was seen after incubation with medium exposed to either PU or cotton functionalized with G or GO ([Figures 4A and 4B](#)).

Material functionalization with G or GO also can protect against the transmission of bacteria. Therefore, we also tested the protective effects of G-integrated materials on *E. coli* growth. Antibacterial efficacy was

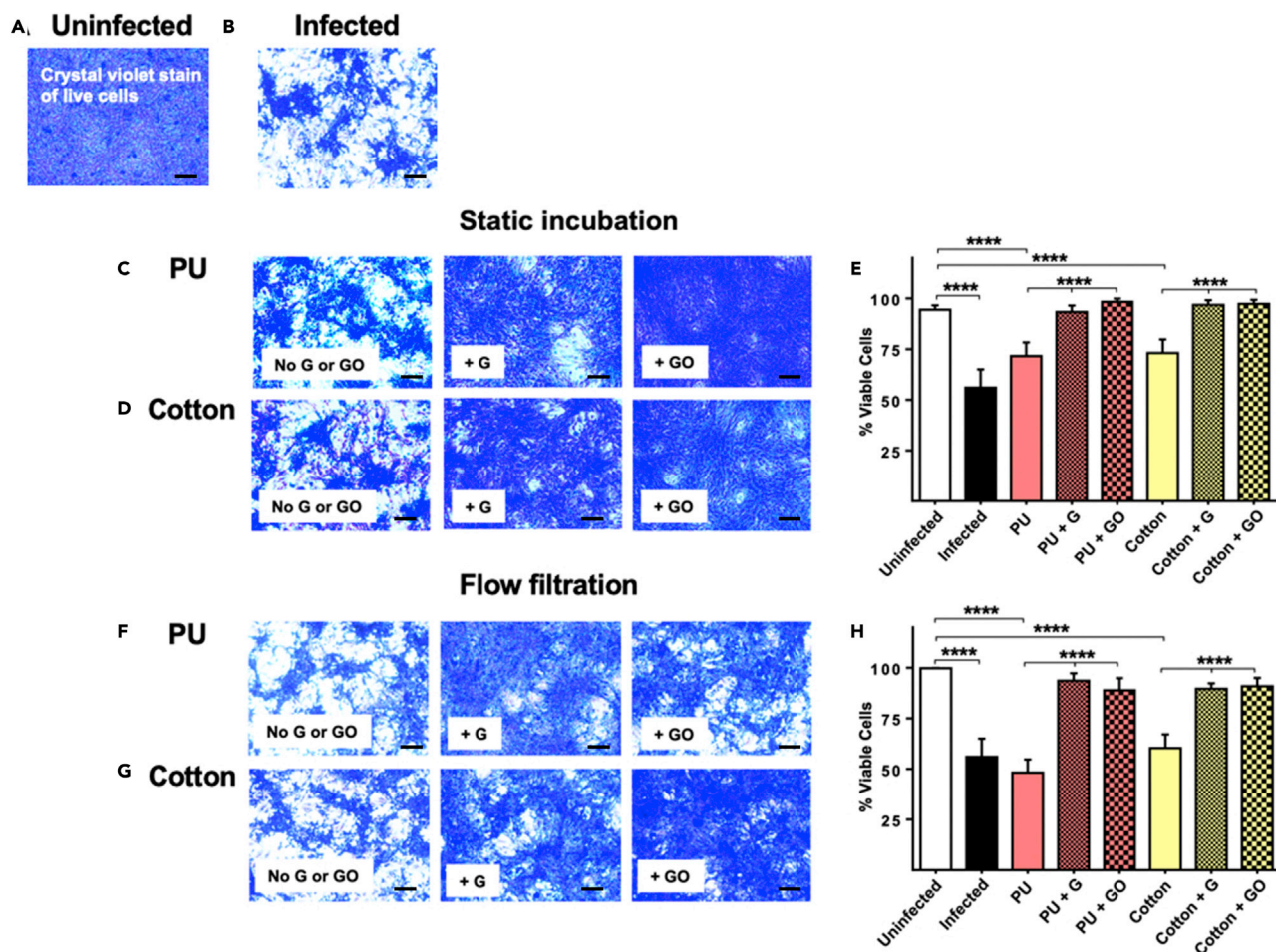


Figure 3. Graphene (G)- and graphene oxide (GO)-functionalized materials inhibit viral infection of VERO cells in static and flow testing paradigms
 (A) Uninfected VERO cells stained with crystal violet are ~100 confluent.
 (B) Similar crystal violet staining of infected cells reveals severe cell loss (white areas).
 (C and D) Representative images of cells exposed to (C) PU or (D) cotton without or with G or GO functionalization and stained with crystal violet in the static incubation experiment are shown.
 (E) Data from quantified crystal violet-stained cell images reveal highly significant increases in cell survival with PU or cotton with G or GO.
 (F and G) Similar representative images are shown for the flow filtration experiment.
 (H) Crystal violet-stained cell image quantification for the flow experiment also shows highly significant increases in cell viability with both materials functionalized with either G or GO. Scale bars in A–D, F, and G are 50 μm . Data are represented as mean \pm SD. Statistically significant results are indicated with “*” according to p value (* $p < 0.05$; ** $p < 0.01$; *** $p < 0.001$; **** $p < 0.0001$).

expressed with value R, which is obtained by $R = U_T - A_T$. U_T is the average of the common logarithm of the number of viable bacteria, in cells/cm², recovered from the untreated test specimens after 24 h; A_T is the average of the common logarithm of the number of viable bacteria, in cells/cm², recovered from the treated test specimens after 24 h.

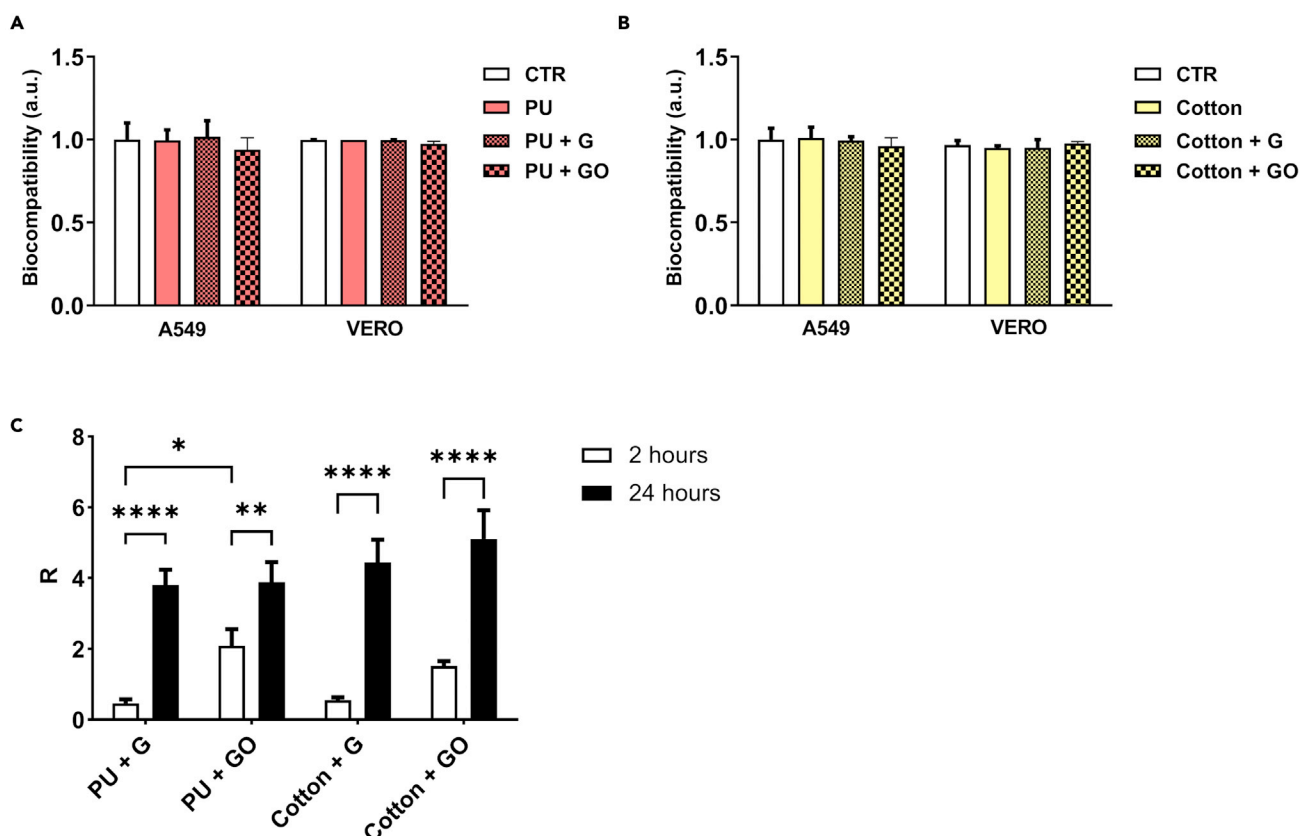
As shown in Figure 4C, after 2 h of incubation with functionalized fabric, *E. coli* growth was reduced on PU-G and cotton-G with an R value of ~0.5 for both; R values were higher for GO- compared with G-functionalized materials. The R value is essentially the difference between viable bacteria in an untreated culture and a treated culture; thus, if fewer bacteria are viable after a given treatment, the R value is increased. After 24 h, the R value was 3.8 and 4.4 for PU with G and cotton with G, respectively, and 3.8 and ~5 for PU with GO and cotton with GO, respectively, indicating a significant inhibition of bacterial growth by both functionalized materials (Figure 4C). These experiments confirm that the contact of microorganisms with carbon materials causes a strong interaction that impedes the release of infectious agents in the environment.

Table 1. Viral load reduction in static and flow filtration experiment for each type of functionalized fabric. Data are represented as mean \pm SD

Static incubation	Viral load reduction (%)	Static incubation	Viral load reduction (%)
PU	27 \pm 6	Cotton	38 \pm 5
PU + G	97 \pm 3	Cotton G+	99 \pm 2
PU + GO	99 \pm 3	Cotton GO	99 \pm 2
Flow filtration	Viral load reduction (%)	Flow filtration	Viral load reduction (%)
PU	0 \pm 5	Cotton	10 \pm 5
PU + G	88 \pm 5	Cotton G+	77 \pm 3
PU + GO	82 \pm 6	Cotton GO	79 \pm 4

The ability of GO to trap pathogens was one of the first properties attributed to this nanomaterial and was reported to result in inhibition of macrophage infection by *Mycobacterium tuberculosis* (De Maio et al., 2019a, 2019b, 2020), as well as bacteriostatic effect on both Gram-positive and Gram-negative bacteria (Palmieri et al., 2018).

In addition to the potential for integration of GO in PPE, the ability of GO to trap infectious viral particles provides an opportunity for the treatment of water effluents from hospitals and municipalities. This may be a critical application of GO technology, given that coronaviruses can maintain viability in sewage and



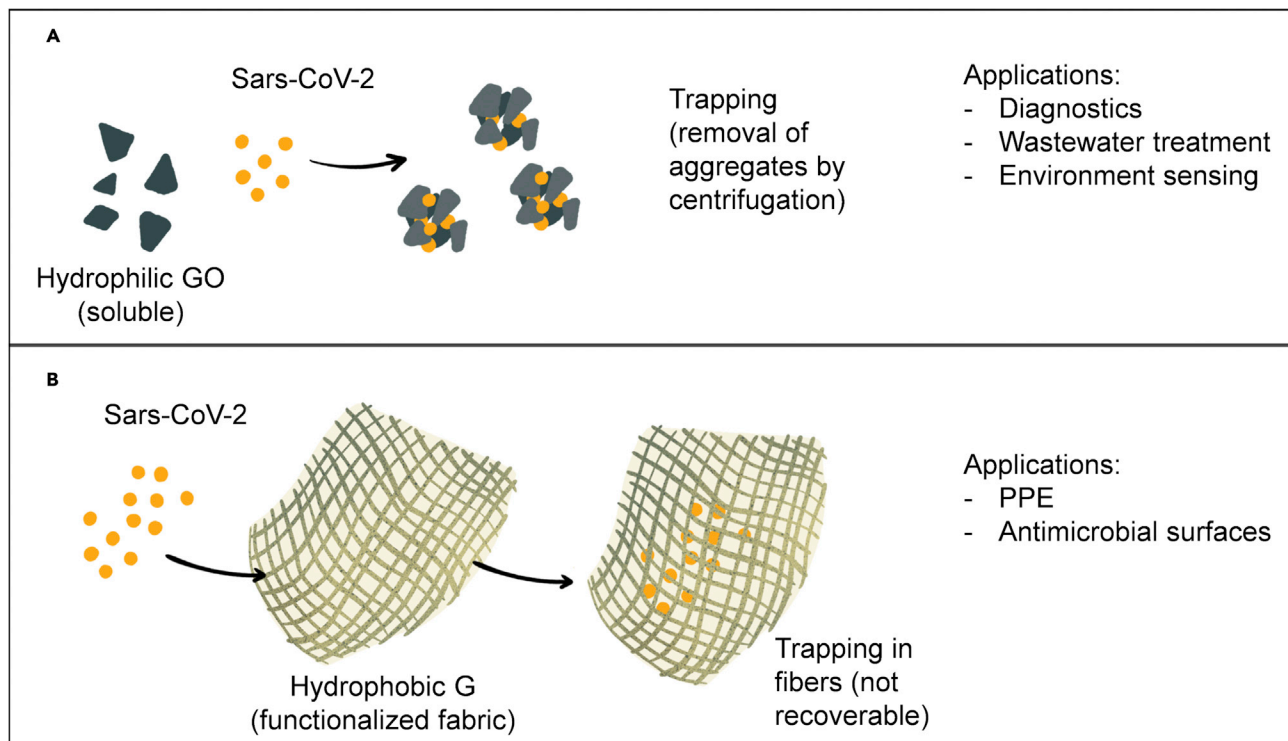


Figure 5. Scheme of application of hydrophilic (GO) in A or hydrophobic (G) materials in B against Sars-CoV-2

hospital wastewater and can persist in aquatic environments and wastewater treatment plants (Naddeo and Liu, 2020). With further development, GO technology could be applied to water treatment and air purification and, in combination with monitoring programs, has the potential to reduce environmental viral loads and secondary transmission.

The GO trapping effect has the potential to be leveraged for other applications; for example, it can be used to concentrate analytes in solution, such as DNA, RNA, and viruses (Palmieri et al., 2020), a feature that is useful for the design of new diagnostic assays.

Although the promising results presented here point to the benefits of either G or GO in PPE material, G and GO are not interchangeable. The hydrophilicity of the material is significantly increased with GO, compared with the hydrophobic G (Figure S2). Depending upon the final design of the face mask incorporating a G- or GO-functionalized material, the first choice may be G if a hydrophobic quality is desired, or GO if the material is positioned between the inner and outer layers where it could trap and neutralize the virus. The more hydrophilic nature of GO makes it a better choice in applications that require solutions such as molecular diagnostic devices or water treatment. In Figure 5, a summary of the main results of the article and of possible exploitation of graphene materials in the future is reported.

CONCLUSIONS

The findings presented in this work support the further development of integration of graphene or graphene oxide into face mask materials given the specific inhibition of live Sars-CoV-2 particles. In our ongoing efforts, we are applying our knowledge of material functionalization (Cesareo et al., 2020) to develop a feasible and practical material with stability to temperature and mechanical or other forces that can be utilized in masks and PPE for widespread use. The routine use of face masks, now encouraged throughout the world where COVID-19 is present, can reduce viral transmissibility and preserve healthcare capacity (Stutt et al., 2020). Graphene and GO nanomaterials present a critical opportunity to increase face mask efficacy, especially in light of the development of multivalent strategies against SARS-CoV-2, bringing the world closer to the goal of stopping the spread of COVID-19 (Tabish and Hamblin, 2020).

STAR★METHODS

Detailed methods are provided in the online version of this paper and include the following:

- KEY RESOURCES TABLE
- RESOURCE AVAILABILITY
 - Lead contact
 - Materials availability
 - Data and code availability
- EXPERIMENTAL MODEL AND SUBJECT DETAIL
 - Cell culture
- METHOD DETAILS
 - G and GO sources
 - GO activity in solution against SARS-CoV-2
 - VERO cell infection
 - Immunofluorescence
 - Cell viability
 - Crystal violet staining
 - Image analysis
 - Functionalization of materials
 - Scanning electron microscopy (SEM)
 - Antiviral effects (flow filtration)
 - Antiviral effects (static conditions)
 - Biocompatibility of functionalized materials
 - Antibacterial properties
- QUANTIFICATION AND STATISTICAL ANALYSIS

SUPPLEMENTAL INFORMATION

Supplemental information can be found online at <https://doi.org/10.1016/j.isci.2021.102788>.

ACKNOWLEDGMENTS

This paper is in memory of G.B., who died prematurely. Work presented in this paper has been partially supported by Directa Plus Srl. Università Cattolica del Sacro Cuore contributed to the funding of this research project and its publication.

AUTHOR CONTRIBUTIONS

This study was designed by F.D.M., V.P., G.D., M. Sali, P.S.-S., and M.P. Infection experiments, and related assays, were performed by F.D.M., I.P., and A.S. Bacteria-based experiments were performed by V.P. and A.A. Electron microscopy was performed by V.P. and A.A. Cell viability experiments were performed by F.D.M. and G.P. Data analysis and figure preparation were conducted by F.D.M., V.P., and G.B. F.D.M., V.P., G.D., M. Sali, P.S.-S., and M.P. wrote the paper. M.D.S. and M. Sanguinetti discussed all the results presented and revised the paper. L.G.R. and G.C. developed and produced graphene nanoplatelets and realized G material functionalization. M.P. and V.P. realized GO material functionalization. All authors read, critically revised, and approved the final manuscript.

DECLARATION OF INTERESTS

L.G.R. and G.C. are both employees of Directa-Plus Srl, and P.S.-S. is a shareholder of Directa-Plus Srl. L.G.R. and G.C. are both inventors for the patents WO2015193267A1 and WO2019202028A1. Other authors declare no competing interests.

Received: April 14, 2021

Revised: June 3, 2021

Accepted: June 22, 2021

Published: July 23, 2021

REFERENCES

- Akhavan, O., Choobtashani, M., and Ghaderi, E. (2012). 'Protein degradation and RNA efflux of viruses photocatalyzed by graphene-tungsten oxide composite under visible light irradiation'. *J. Phys. Chem. C* 116, 9653–9659.
- Ammerman, N.C., Beier-Sexton, M., and Azad, A.F. (2008). Growth and maintenance of Vero cell lines. *Curr. Protoc. Microbiol.* 11, A-4E.
- Arons, M.M., Hatfield, K.M., Reddy, S.C., Kimball, A., James, A., Jacobs, J.R., Taylor, J., Spicer, K., Bardossy, A.C., Oakley, L.P., et al. (2020). Presymptomatic SARS-CoV-2 infections and transmission in a skilled nursing facility. *N. Engl. J. Med.* 382, 2081–2090.
- Bonetti, L., Fiorati, A., Serafini, A., Masotti, G., Tana, F., D'Agostino, A., Draghi, L., Altomare, L., Chiesa, R., Farè, S., et al. (2021). Graphene nanoplatelets composite membranes for thermal comfort enhancement in performance textiles. *J. Appl. Polym. Sci.* 138, 49645.
- Bourque, A.J., and Rutledge, G.C. (2018). Empirical potential for molecular simulation of graphene nanoplatelets. *J. Chem. Phys.* 148, 144709.
- Cesareo, G., Parrini, M.R., and Rizzi, L.G. (2020). Continuous Process for Preparing Pristine Graphene Nanoplatelets (Google Patents).
- Chen, Y.N., Hsueh, Y.H., Hsieh, C.T., Tzou, D.Y., and Chang, P.L. (2016). 'Antiviral activity of graphene-silver nanocomposites against non-enveloped and enveloped viruses'. *Int. J. Environ. Res. Public Health* 13, 430.
- Donskyi, I.S., Azab, W., Cuellar-Camacho, J.L., Guday, G., Lippitz, A., Unger, W.E.S., Osterrieder, K., Adeli, M., and Haag, R. (2019). Functionalized nanographene sheets with high antiviral activity through synergistic electrostatic and hydrophobic interactions. *Nanoscale* 11, 15804–15809.
- Feng, S., Shen, C., Xia, N., Song, W., Fan, M., and Cowling, B.J. (2020). Rational use of face masks in the COVID-19 pandemic. *Lancet Respir. Med.* 8, 434–436.
- Frost, R., Jönsson, G.E., Chakarov, D., Svedhem, S., and Kasemo, B. (2012). Graphene oxide and lipid membranes: interactions and nanocomposite structures. *Nano Lett.* 12, 3356–3362.
- Jones, S.T., Cagno, V., Janeček, M., Ortiz, D., Gasilova, N., Piret, J., Gasbarri, M., Constant, D.A., Han, Y., Vuković, L., et al. (2020). Modified cyclodextrins as broad-spectrum antivirals. *Sci. Adv.* 6, eaax9318.
- Kumar, A., Sharma, K., and Dixit, A.R. (2020). Role of graphene in biosensor and protective textile against viruses. *Med. Hypotheses* 144, 110253.
- Kumar, S., and Parekh, S.H. (2020). Linking graphene-based material physicochemical properties with molecular adsorption, structure and cell fate. *Commun. Chem.* 3, 1–11.
- Lin, Z., Wang, Z., Zhang, X., and Diao, D. (2020). Superhydrophobic, photo-sterilize, and reusable mask based on graphene nanosheet-embedded carbon (GNEC) film. *Nano Res.* 1–14.
- Liu, Z., Chu, R., Gong, L., Su, B., and Wu, J. (2020). The assessment of transmission efficiency and latent infection period in asymptomatic carriers of SARS-CoV-2 infection. *Int. J. Infect. Dis.* 99, 325–327.
- Clase, C.M., Fu, E.L., Joseph, M., Beale, R.C., Dolovich, M.B., Jardine, M., Mann, M.F., Pecoits-Filho, R., Winkelmayer, W.C., and Carrero, J.J. (2020). Cloth Masks May Prevent Transmission of COVID-19: An Evidence-Based, Risk-Based Approach (American College of Physicians), pp. M20–M2567.
- De Maio, F., Maulucci, G., Minerva, M., Anosheh, S., Palucci, I., Iantomasi, R., Palmieri, V., Camassa, S., Sali, M., Sanguinetti, M., et al. (2014). Impact of protein domains on PE_PGRS30 polar localization in Mycobacteria. *PLoS One* 9, e112482.
- De Maio, F., Palmieri, V., De Spirito, M., Delogu, G., and Papi, M. (2019a). Carbon nanomaterials: a new way against tuberculosis. *Expert Rev. Med. Devices* 16, 863–875.
- De Maio, F., Palmieri, V., Salustri, A., Perini, G., Sanguinetti, M., De Spirito, M., Delogu, G., and Papi, M. (2019b). Graphene oxide prevents mycobacteria entry into macrophages through extracellular entrapment. *Nanoscale Adv.* 1, 1421–1431.
- De Maio, F., Palmieri, V., Santarelli, G., Perini, G., Salustri, A., Palucci, I., Sali, M., Gervasoni, J., Primiano, A., Ciasca, G., et al. (2020). Graphene oxide-linezolid combination as potential new anti-tuberculosis treatment. *Nanomaterials* 10, 1431.
- Matharu, R.K., Porwal, H., Chen, B., Ciric, L., and Edirisinghe, M. (2020). 'Viral filtration using carbon-based materials'. *Med. Devices Sens* 3, e10107.
- Naddeo, V., and Liu, H. (2020). Editorial Perspectives: 2019 novel coronavirus (SARS-CoV-2): what is its fate in urban water cycle and how can the water research community respond? *Environ. Sci. Water Res. Technol.* 6, 1213–1216.
- Naskalska, A., Dabrowska, A., Szczepanski, A., Milewska, A., Jasik, K.P., and Pyrc, K. (2019). Membrane protein of human coronavirus NL63 is responsible for interaction with the adhesion receptor. *J. Virol.* 93, e00355–19.
- Palmieri, V., Bugli, F., Lauriola, M.C., Cacaci, M., Torelli, R., Ciasca, G., Conti, C., Sanguinetti, M., Papi, M., and De Spirito, M. (2017a). Bacteria meet graphene: modulation of graphene oxide nanosheet interaction with human pathogens for effective antimicrobial therapy. *ACS Biomater. Sci. Eng.* 3, 619–627.
- O'Dowd, K., Nair, K.M., Forouzandeh, P., Mathew, S., Grant, J., Moran, R., Bartlett, J., Bird, J., Pillai, S.C., et al. (2020). Face masks and respirators in the fight against the COVID-19 pandemic: a review of current materials, Advances and Future perspectives. *Materials* 13, 3363.
- Palmieri, V., Barba, M., Di Pietro, L., Gentilini, S., Braidotti, M.C., Ciancico, C., Bugli, F., Ciasca, G., Larciprete, R., Lattanzi, W., et al. (2017b). Reduction and shaping of graphene-oxide by laser-printing for controlled bone tissue regeneration and bacterial killing. *2d Mater.* 5, 015027.
- Palmieri, V., Carmela Lauriola, M., Ciasca, G., Conti, C., De Spirito, M., and Papi, M. (2017c). The graphene oxide contradictory effects against human pathogens. *Nanotechnology* 28, 152001. <https://doi.org/10.1088/1361-6528/aa6150>.
- Palmieri, V., Bugli, F., Cacaci, M., Perini, G., Maio, F., Delogu, G., Torelli, R., Conti, C., Sanguinetti, M., Spirito, M., et al. (2018). Graphene oxide coatings prevent *Candida albicans* biofilm formation with a controlled release of curcumin-loaded nanocomposites. *Nanomedicine (Lond)* 13, 2867–2879. <https://doi.org/10.2217/nnm-2018-0183>.
- Palmieri, V., Di Pietro, L., Perini, G., Barba, M., Parolini, O., De Spirito, M., Lattanzi, W., and Papi, M. (2020). Graphene oxide nano-concentrators selectively modulate RNA trapping according to metal cations in solution. *Front. Bioeng. Biotechnol.* 8, 421.
- Palmieri, V., De Maio, F., De Spirito, M., and Papi, M. (2021). Face masks and nanotechnology: keep the blue side up. *Nano Today* 37, 101077.
- Palmieri, V., and Papi, M. (2020). Can graphene take part in the fight against COVID-19? *Nano Today* 33, 100883.
- Raghav, P.K., and Mohanty, S. (2020). Are graphene and graphene-derived products capable of preventing COVID-19 infection? *Med. Hypotheses* 144, 110031.
- Rizzi, L.G., Cesareo, G., and Popescu, R. (2021). Textile Article Comprising Graphene and Process for its Preparation (Google Patents).
- Rui, L., Liu, J., Li, J., Weng, Y., Dou, Y., Yuan, B., Yang, K., and Ma, Y. (2015). Reduced graphene oxide directed self-assembly of phospholipid monolayers in liquid and gel phases. *Biochim. Biophys. Acta* 1848, 1203–1211.
- Sarkar, S., Mukhopadhyay, A., Sen, S., Mondal, S., Banerjee, A., Mandal, P., Ghosh, R., Megaridis, C.M., Ganguly, R., et al. (2020). Leveraging Wettability Engineering to Develop Three-Layer DIY Face Masks from Low-Cost Materials (Transactions of the Indian National Academy of Engineering), p. 1.
- Shams, E., Yeganeh, H., Naderi-Manesh, H., Gharibi, R., and Mohammad Hassan, Z. (2017). Polyurethane/siloxane membranes containing graphene oxide nanoplatelets as antimicrobial wound dressings: in vitro and in vivo evaluations. *J. Mater. Sci. Mater. Med.* 28, 75.
- Sommerstein, R., Fux, C.A., Vuichard-Gysin, D., Abbas, M., Abbas, J., Balmelli, C., Troillet, N., Harbarth, S., Schlegel, M., Widmer, A., et al. (2020). Risk of SARS-CoV-2 transmission by aerosols, the rational use of masks, and protection of healthcare workers from COVID-19. *Antimicrob. Resist. Infect. Control* 9, 1–8.
- Song, Z., Wang, X., Zhu, G., Nian, Q., Zhou, H., Yang, D., Qin, C., and Tang, R. (2015). Virus capture and destruction by label-free graphene oxide for detection and disinfection applications. *Small* 11, 1171–1176.

Sportelli, M.C., Izzi, M., Kukushkina, E.A., Hossain, S.I., Picca, R.A., Ditaranto, N., and Cioffi, N. (2020). Can nanotechnology and materials science help the fight against SARS-CoV-2? *Nanomaterials* *10*, 802.

Srivastava, A.K., Dwivedi, N., Dhand, C., Khan, R., Sathish, N., Gupta, M.K., Kumar, R., and Kumar, S. (2020). Potential of graphene-based materials to combat COVID-19: properties, perspectives and Prospects. *Mater. Today Chem.* *18*, 100385.

Stutt, R.O.J.H., Retkute, R., Bradley, M., Gilligan, C.A., and Colvin, J. (2020). A modelling framework to assess the likely effectiveness of facemasks in combination with 'lock-down' in managing the COVID-19 pandemic. *Proc. R. Soc. A* *476*, 20200376.

Sunjaya, A.P., and Jenkins, C. (2020). Rationale for universal face masks in public against COVID-19. *Respirology* *25*, 678–679.

Tabish, T.A., and Hamblin, M.R. (2020). Multivalent nanomedicines to treat COVID-19: a slow train coming. *Nano Today* *35*, 100962.

Valentini, L., Bittolo Bon, S., Signetti, S., and Pugno, N.M. (2016). Graphene-based bionic

composites with multifunctional and repairing properties. *ACS Appl. Mater. Interfaces* *8*, 7607–7612.

Wang, M., Niu, Y., Zhou, J., Wen, H., Zhang, Z., Luo, D., Gao, D., Yang, J., Liang, D., and Li, Y. (2016). The dispersion and aggregation of graphene oxide in aqueous media. *Nanoscale* *8*, 14587–14592.

Weiss, C., Carriere, M., Fusco, L., Capua, I., Regla-Nava, J.A., Pasquali, M., Scott, J.A., Vitale, F., Unal, M.A., Mattevi, C., et al. (2020). Toward nanotechnology-enabled approaches against the COVID-19 pandemic. *ACS Nano* *14*, 6383–6406.

Yang, X.X., Li, C.M., Li, Y.F., Wang, J., and Huang, C.Z. (2017). Synergistic antiviral effect of curcumin functionalized graphene oxide against respiratory syncytial virus infection. *Nanoscale* *9*, 16086–16092.

Zhao, J., Deng, B., Lv, M., Li, J., Zhang, Y., Jiang, H., Peng, C., Li, J., Shi, J., Huang, Q., and Fan, C. (2013). Graphene oxide-based antibacterial cotton fabrics. *Adv. Healthc. Mater.* *2*, 1259–1266.

Zhiqing, L., Yongyun, C., Wenxiang, C., Mengning, Y., Yuanqing, M., Zhenan, Z., Haishan, W., Jie, Z., Kerong, D., Huiwu, L., et al. (2018). Surgical masks as source of bacterial contamination during operative procedures. *J. Orthop. Translat.* *14*, 57–62.

Zhong, H., Zhu, Z., Lin, J., Cheung, C.F., Lu, V.L., Yan, F., Chan, C.Y., and Li, G. (2020). Reusable and recyclable graphene masks with outstanding superhydrophobic and photothermal performances. *ACS Nano* *14*, 6213–6221.

Ziem, B., Thien, H., Achazi, K., Yue, C., Stern, D., Silberreis, K., Gholami, M.F., Beckert, F., Gröger, D., Mülhaupt, R., et al. (2016). Highly efficient multivalent 2D nanosystems for inhibition of orthopoxvirus particles. *Adv. Healthc. Mater.* *5*, 2922–2930.

Ziem, B., Azab, W., Gholami, M.F., Rabe, J.P., Osterrieder, N., and Haag, R. (2017). Size-dependent inhibition of herpesvirus cellular entry by polyvalent nanoarchitectures. *Nanoscale* *9*, 3774–3783.

STAR★METHODS

KEY RESOURCES TABLE

REAGENT or RESOURCE	SOURCE	IDENTIFIER
Antibodies		
Monoclonal rabbit anti-Spike S1 subunit antibodies	Novusbio	clone CR3022
secondary anti-rabbit IgG - FITC labelled antibodies	Invitrogen	Ref: 65-6111/ lot: UG285467
Bacterial and virus strains		
SARS-CoV-2	Clinical isolate	-
<i>E. coli</i>	ATCC	25922
Chemicals, peptides, and recombinant proteins		
Graphene Oxide (GO)	GrapheneA	C990/GOB105/D
Paraformaldehyde	ChemCruz	Sc-281692
DMEM	EuroClone	P04-03500
PBS	EuroClone	ECB4004L
L-glutamine	EuroClone	ECB3000D
Streptomycin - Penicillin	EuroClone	ECB3001D
Trypsin/EDTA	EuroClone	P10-023100
Triton X-100	Sigma	T-9284
Cristal Violet	RC	29524
Bovine serum albumin	Sigma	A4503-100G
Critical commercial assays		
LDH assay	Lonza	MK401-2
MTT assay (3-(4,5-dimethylthiazol-2-yl)-2,5-diphenyltetrazolium bromide)	Invitrogen, Life technologies	Lot 2246601/Ref V13154
Deposited data		
All data reported in this paper will be shared by the lead contact upon request.		
Experimental models: Cell lines		
VERO	ATCC	CCL-81
A549 lung cancer cells	ATCC	CCL-185
Software and algorithms		
FIJI	ImageJ 1.53c	https://imagej.net/software/fiji/
Microsoft Excel 2016	Microsoft Office	https://www.office.com/
GraphPad Prism 8.0 software	GraphPad	https://www.graphpad.com/scientific-software/prism/

RESOURCE AVAILABILITY

Lead contact

Further information and requests for resources and reagents should be directed to and will be fulfilled by the lead contact, Massimiliano Papi (massimilianopapi@unicatt.it).

Materials availability

This study did not generate new unique reagents.

Data and code availability

All data reported in this paper will be shared by the lead contact upon request. This paper does not report original code. Any additional information required to reanalyze the data reported in this paper is available from the lead contact upon request.

EXPERIMENTAL MODEL AND SUBJECT DETAIL

Cell culture

African green monkey kidney (VERO) epithelial cells (ATCC CCL-81 sex of cell Female) were cultured in Dulbecco's Modified Eagle's Medium (DMEM) supplemented with 10% inactivated fetal calf serum (FCS) (EuroClone, Milan, Italy), 1 mM glutamine (EuroClone, Milan, Italy), 1% streptomycin - penicillin antibiotics (EuroClone, Milan, Italy) and incubated in a humidified atmosphere (5% CO₂ at 37°C) as reported elsewhere (Ammerman et al., 2008). Cells were washed with sterile warm phosphate buffered saline (PBS), trypsinized and counted. Cells were replated in 48-well plates (Wuxi NEST Biotechnology Co., Ltd, China) at 7 × 10⁴ cells/mL. Cells were infected with SARS-CoV-2 virus when > 90% confluent monolayer was observed comprising approximately 1 × 10⁶ cells/well after 72 hours. A549 cells (ATCC sex of cell male) were maintained in DMEM (Sigma-Aldrich) supplemented with 10% fetal bovine serum (FBS, EuroClone), 2% penicillin-streptomycin (Sigma-Aldrich) and 2% L-glutamine (Sigma-Aldrich). Cells were cultivated in T75 flasks and kept at 37°C in 5% CO₂ humidity. Biocompatibility test has been performed also on VERO cells using cell culture conditions specified above.

METHOD DETAILS

G and GO sources

G (G+, Directa Plus) and GO (GO, GrapheneA) were used for all experiments. Commercial materials were used to ensure consistency between experiments. G+ is produced according to a proprietary patented technology that involves three different steps: expansion, exfoliation, and drying (Bonetti et al., 2021). GO water dispersion (4 mg/mL) synthesis was performed using the Hummers' method (Wang et al., 2016). In the Table S1, the main parameters for each nanomaterial are summarized. Full characterization of these nanomaterials is reported elsewhere (Palmieri et al., 2017b; Cesareo et al., 2020).

GO activity in solution against SARS-CoV-2

To assay the ability of GO to trap SARS-CoV-2, we incubated previously titred SARS-CoV-2 particles in suspension with GO diluted in phosphate buffered saline (PBS) supplemented with 1% penicillin – streptomycin. Briefly, 0.06, 0.12, 0.25, and 0.5 mg/mL of GO were incubated with SARS-CoV-2 virus (~10⁵ virus particles/mL). Incubation was performed at 37°C with agitation (100 rpm). Two hours later, GO was removed by centrifugation (14,000 rpm, 5 minutes) and supernatant was used to infect VERO cells (Figure 1A). The cytopathic effect of SARS-CoV-2 was evaluated 72 hours after the infection including full-spectrum light microscopy and image collection for quantification of area covered by viable cells labelled with crystal violet staining. Further infection evaluation was done by labeling of SARS-CoV-2 particles with an anti-spike antibody and performing lactate dehydrogenase (LDH) assay, all described below.

VERO cell infection

To initiate infection, cells were washed with sterile warm PBS and then infected with 0.1 mL of solution containing SARS-CoV-2 (~10⁵ virus particles/mL). Cells were incubated for two hours at standard atmosphere conditions (37°C, 5% CO₂), then the infection solution was removed and replaced with fresh DMEM medium supplemented with 2% FCS, 1 mM glutamine, and 1% streptomycin - penicillin as above. Cells were incubated and infection status was evaluated daily. All experiments that involved SARS-CoV-2 manipulation was carried out in Biosafety level 3 laboratory (BSL3) in the Institute of Microbiology of IRCCS – Fondazione Policlinico Gemelli.

Immunofluorescence

IF was performed to assess viral replication in VERO cells. Cells were fixed by using 4% paraformaldehyde for 30 minutes. After three washes, fixed cells were permeabilized (0.02% Triton X-100 in PBS) and a blocking step was performed by using PBS supplemented with 0.3% bovine serum albumin (BSA) (De Maio et al., 2014). SARS-CoV-2 viral particles were labelled with monoclonal rabbit anti-Spike S1 subunit antibodies (Novusbio, clone CR3022), the plate was incubated for 3 hours at room temperature, and after washes

with PBST, incubated with secondary anti-rabbit IgG - FITC labelled antibodies (Ref: 65-6111/ lot: UG285467, Invitrogen). The fluorescent signal was detected by using a Nikon eclipse TS100 and images used for quantification of the signal as described below.

Cell viability

To evaluate cell viability, LDH levels in cell culture media supernatants were determined. Each supernatant was diluted according to the LDH kit manufacturer's instructions (LONZA) before incubation with the substrate. Thirty minutes later absorbance at 450 nm was measured with a plate reader (BioRad).

Crystal violet staining

Crystal violet labels the DNA of live, adherent cells and was used to quantify viable cells. Cells were fixed as described above and then stained by using Crystal violet for 30 minutes. After incubation, five washes were carried out and images of random fields for each condition were acquired and the stain signal quantified as described below.

Image analysis

Images were analyzed using open-access ImageJ software version 1.47v (NIH, USA). Every set of .tiff images corresponding to crystal violet staining were analyzed through the "Process>Batch>Macro tool". Each image was converted to 8-bit image. Minimum and Maximum thresholds were manually set for each batch of images to correctly convert areas to white and black, respectively. Prior to perform the "Measure" tool of ImageJ, images were processed with the "Smooth" and "Convert to Mask". The fraction of the area covered by cells is then automatically stored in the results file. IF images were generated by merging image of cells acquired with direct light and the corresponding image acquired with 476 nm light (UV) by ImageJ software built-in tool "Image>Color>Merge" using the grey and green channels, respectively.

Functionalization of materials

Polyurethane (PU) and cotton materials were functionalized with G+ or GO as previously described (Zhao et al., 2013; Rizzi et al., 2021).

Scanning electron microscopy (SEM)

SEM was performed to evaluate graphene and GO distribution on materials. A piece of each material was cut (1x1 cm) and sputter-coated with platinum then imaged with SEM Supra 25 (Zeiss, Germany). Images were acquired at several magnifications.

Antiviral effects (flow filtration)

A 3D printed custom sample holder was produced using Ultimaker S3 to hold material samples. SARS-CoV-2 infection solution was prepared as indicated above and 1 mL was filtered through the device containing the material. Positive and negative controls are represented by infection solution and sterile PBS passed through empty filters, respectively. 0.1 mL of each eluate was used to infect VERO cells as indicated above. The cytopathic effect was evaluated at 72 hours after the infection.

Antiviral effects (static conditions)

The antiviral property of materials was evaluated following ISO18184 procedures. 0.05 mL of PBS containing SARS-CoV-2 virus was put on the surface of a 1x1 cm² textile TNT and cotton and corresponding graphene functionalized materials. After two hours of incubation, each material was recovered in a new tube containing 5 ml of DMEM supplemented with 2% inactivated FCS, 1 mM glutamine, 1% streptomycin - penicillin antibiotics. Additionally, 0.1 mL was used to wash and to collect infection solution in the wells containing the materials. Each tube containing infected material was vigorously vortexed five times and 0.1 mL was used to infect VERO cells as described above. The cytopathic effect was monitored daily by visual inspection.

Biocompatibility of functionalized materials

To assess if the cotton or PU materials functionalized with G or GO were toxic to cells, in the absence of virus, A549 lung cancer cells and VERO cells were incubated with material-exposed medium.

Material biocompatibility was evaluated according to ISO 10993. Material pieces (2 x 2 cm) were incubated in 10 mL of complete medium at 37°C for 24 hours. Meanwhile, cells were seeded on 96-well (Corning) at a density of 10⁵ cells/mL, and kept at 37°C in 5% CO₂ humidity for 24 hours. After incubation, supernatant in the multiwell was aspirated and replaced with 100 μL of culture medium incubated with functionalized materials. Cells were then kept at 37°C in 5% CO₂ humidity. After 24 hours, MTT assay (3-(4,5-dimethylthiazol-2-yl)-2,5-diphenyltetrazolium bromide (Invitrogen, Life technologies, Italy)) was performed. Briefly, culture medium was removed and replaced with fresh medium containing 12 mM MTT. Cells were incubated for 4 hours at 37°C in 5% CO₂ humidity. After incubation, 100 μL of component B (1 mg of sodium dodecyl sulfate in 10 mL of 0.01 M HCl) per 100 μL of medium was added to each well, and incubated for 16 hours. Absorbance was read at 570 nm with a microplate reader (Cytation3, Biotek) and results were normalized by control cells.

Antibacterial properties

E. coli (ATCC 25922) was used to perform tests of antibacterial effects of materials according to ISO 20743:2013 using a colony plate count method. Cotton or PU without G or GO were used as control materials to validate the growth condition of test bacteria and validate the test. Bacteria were grown in sterile Luria-Broth (LB) medium at 37°C overnight. A sub-inoculum of the bacteria was grown until a logarithmic phase of growth was achieved and diluted to a concentration of 10⁵ cells/mL. Material test specimens were cut in pieces (2 cm x 2 cm) and incubated with 200 μL of bacterial suspension and incubated at 37°C. Bacteria were retrieved from each specimen at several time points to count colony forming units (CFU) on LB agar plates. Antibacterial efficacy is expressed with R value which is obtained by $R = U_T - A_T$. U_T is the average of the common logarithm of the number of viable bacteria, in cells/cm², recovered from the untreated test specimens after 24 h; A_T is the average of the common logarithm of the number of viable bacteria, in cells/cm², recovered from the treated test specimens after 24 h. All tests were performed in triplicate.

QUANTIFICATION AND STATISTICAL ANALYSIS

All experiments have been replicated at least three times. Microsoft Excel 2010 (Microsoft Office) and GraphPad Prism 8.0 software (GraphPad) were used to compile and analyze data. All data are expressed as mean with standard deviation (SD) and analyzed by one-way ANOVA comparison tests followed by Tukey's correction. Statistically significant results are indicated with "*" according to p value ($p < 0.05 = *$; $p < 0.01 = **$; $p < 0.001 = ***$; $p < 0.0001 = ****$). Statistical methods details can be found in the Figure Legends.